Scientific report

by Prof. **Ya. S. Greenberg**

Visit to IPHT (Jena, Germany) from 17 July 2006 to 28 August 2006
under ESF grant 1030

1. Purpose of the visit

The visit was aimed at the further development of scientific collaboration with the IPHT team involving in the number of European qubit projects. The main purpose of the visit was the development of the new theoretical methods for the characterization of superconducting qubits and for their applications as quantum detectors.

2. The work carried out during the visit

A) The interaction of a dissipative two level quantum system (TLS) with high and low frequency excitation has been analyzed in the frame of dressed state approach. In the frame of this approach the method of low frequency Rabi spectroscopy for the dissipative TLS has been developed in application to the flux and charge qubits.

B) The possibility for the application of the flux qubit as a quantum limited magnetometer has been analyzed.

3. The main results obtained

A) In the frame of dressed state approach there have been developed a method for the calculation of low frequency Rabi susceptibilities for dissipative TLS interacting with the high frequency photon field. The Bloch equations in the basis of dressed states for the reduced density matrix have been obtained from the rate equations for the primary density matrix. The analytic solution to these Bloch equations has been obtained for the case of a weak low frequency excitation. The solution allows for the calculation of the low frequency susceptibilities of the system.

B) The voltage-to-flux and phase-to-flux transfer functions for the flux qubit have been calculated, the main noise sources have been studied and it was shown that the ultimate sensitivity of the flux qubit can be as low as 10^{-7} $\Phi_0/\text{Hz}^{1/2}$, that is an order of magnitude better than the best figures for the conventional SQUID magnetometers.
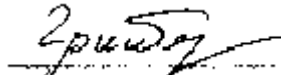
4. Projected publications

During the visit two papers which are assumed to be published in refereeing journals have been prepared. The papers are posted to e-print archive:

1. E. Il'ichev and Ya. S. Greenberg, *Flux qubit as a sensor for a magnetometer with quantum limited sensitivity*, e-print archive cond-mat/0608416. The paper is submitted for publication in Applied Physics Letters.

2. Ya. S. Greenberg, *Low frequency Rabi spectroscopy of dissipative two level systems. The dressed state approach*, e-print archive cond-mat/0609144. The paper is now being prepared for the submitting to Physical Review B for publication as a regular article.

These two preprints are attached to the report.

5. Future collaboration with IPHT in the frame of qubit projects is envisaged.

07. 09.2006   Ya, S. Greenberg

Low frequency Rabi spectroscopy of dissipative two level systems. The dressed state approach.

Ya. S. Greenberg

Novosibirsk State Technical University, 20 K. Marx Ave., 630092 Novosibirsk, Russia.

(Dated: September 7, 2006)

We have analyzed the interaction of a dissipative two level quantum system (TLS) with high and low frequency excitation. The interaction of TLS with high frequency excitation is considered in the frame of dressed state approach. The level structure of the combined TLS+high frequency field system consists of manifolds the spacing between two levels in a given manyfold being equal to Rabi frequency. If the low frequency signal is tuned to the Rabi frequency then the response of the system exhibits an undamped low frequency oscillations, whose amplitude has a clear resonance at the Rabi frequency with the width being dependent on the damping rates of the system. The method can be useful for low-frequency Rabi spectroscopy in various physical systems which are described by a two-level Hamiltonian, such as nuclei spins in NMR, double well quantum dots, superconducting flux and charge qubits, etc.

I. INTRODUCTION

It is well known that under resonant irradiation a quantum two-level system (TLS) can undergo coherent (Rabi) oscillations. The frequency of these oscillations is proportional to the amplitude of the resonant field[1] and is much lower than the gap frequency of TLS. The effect is widely used in molecular beam spectroscopy[2], and in quantum optics[3].

During the last several years it has been proven experimentally that Rabi spectroscopy can serve as a valuable tool for the determination of relaxation times in solid-state quantum mechanical two-level systems, qubits, to be used for quantum information processing[4]. These systems normally are strongly coupled to the environment, which results in the fast damping of Rabi oscillations. It prevents the use of conventional continuous measurements schemes for their detection, though the special schemes for the detection of coherent oscillations through a weak continuous measurement of a TLS were proposed in[5,6,7]. That is why Rabi oscillations are measured with the pulse technique through the statistic of switching events of the occupation probability between two energy levels with excitation and readout being taken at the gap frequency of TLS, which normally, lies in GHz range[8,9,10,11].

Recent successful development of the method of low frequency characterization of the flux qubits by a weak continuous measurements in the radio frequency domain (see review paper[12] and references therein) allowed for the first spectroscopic monitoring of Rabi oscillations with the low-frequency tank circuit which has been tuned to the Rabi frequency of the flux qubit[13]. These experiments stimulated theorists to study the different methods for the detection of Rabi oscillations with the aid of low frequency (compared to the energy gap between two levels) electronic circuitry[14,15,16].

One of the methods for the detection of Rabi resonance at low frequencies has been suggested in papers[17,18]. The method consists in irradiating a TLS continuously by two external sources. The first source with a frequency ω_0, which is close to the energy gap between the two levels, excites the low-frequency Rabi oscillations. Normally, Rabi oscillations are damped out with a rate, which is dependent on how strongly the system is coupled to the environment. However, if a second low-frequency source is applied simultaneously to TLS it responds with persistent low frequency oscillations. The amplitude of these low-frequency oscillations has a resonance at the Rabi frequency with the width being dependent on the damping rates of the system. In papers[17,18] we analyzed the Bloch equations for the quantities $\langle \sigma_Z \rangle$, $\langle \sigma_Y \rangle$, $\langle \sigma_X \rangle$, where brackets denote the averaging over environmental degrees of freedom. Two external sources at high and low frequency were incorporated in the structure of Bloch equations from the very beginning. We showed analytically as well as by direct computer simulations of the Bloch equations that the quantities $\langle \sigma_Z \rangle$, $\langle \sigma_Y \rangle$, $\langle \sigma_X \rangle$ exhibit undamping oscillations with resonance at the Rabi frequency.

The present paper differs from[17,18] in that we study the problem within a dressed state approach, which is well known in quantum optics[19]. We show that, as distinct from the quantum optics, in dissipative solid state TLS there exists interaction which can induce the transitions between the dressed Rabi levels. These transitions result in the low frequency response of the system with the resonance being at the Rabi frequency. We derive the Bloch equations for the elements of reduced density matrix and find the low frequency susceptibilities of the coupled system TLS+photon field.

The paper is organized as follows. In Section II we consider TLS interacting with a one mode laser field which is tuned to the gap of TLS. The structure of energy levels of the global system (TLS+laser field) consists of manifolds the spacing between two levels in a given manyfold being equal to Rabi frequency. We write down the wave functions for these two levels and calculate the transi-

tion amplitudes between them which result from the low frequency excitation. In Second III we define the density matrix in uncoupled basis and write down the phenomenological rate equations for the elements of the density matrix. In Section IV the density matrix in the basis of the dressed states is defined and the rate equations for the element of the density matrix traced over the photon number N are derived. In Section V we rewrite the rate equations for the reduced density matrix in such a way that their structure is similar to that of Bloch equations. For the case of small high frequency detuning the steady state solutions to these equations are found. In Section VI the Bloch equations are modified to include the low frequency excitation. The low frequency susceptibilities for the coupled TLS+photon field system are found in the section both for arbitrary and small high frequency detuning.

II. INTERACTION OF TLS WITH A LASER FIELD IN THE PICTURE OF DRESSED STATES

We start from Hamiltonian of two level system (TLS) subjected to high frequency field:

$$H = \frac{\Delta}{2}\sigma_x + \frac{\varepsilon}{2}\sigma_z + \hbar\omega_0(a^+a + 1/2) + H_{int} \quad (1)$$

Here the first two terms describe an isolated TLS, which can model a great variety of situations in physics and chemistry: from a spin-(1/2) particle in a magnetic field to superconducting flux and charge qubits[4,20]. In order to be exact we consider the TLS in (1) to describe a double-well system where only the ground states of the two wells are occupied, with Δ being the energy splitting of a symmetric ($\varepsilon = 0$) TLS due to quantum tunnelling between two wells. The quantity ε is the bias, the external energy parameter which makes the system asymmetric. The third term in (1) is the Hamiltonian of the laser mode, a^+ and a being creation and annihilation operators. The last term in (1) describes the interaction of TLS with a laser field. This interaction modulates the energy asymmetry between the two wells.

$$H_{int} = -\sigma_z F(a^+ + a) \quad (2)$$

Hamiltonian of TLS in (1) is written in the localized state basis, i.e., in the basis of states localized in each well. In terms of the eigenstates basis, which we denote by upper-case subscripts for the Pauli matrices $\sigma_X, \sigma_Y, \sigma_Z$, Hamiltonian (1) reads

$$H = \frac{\Delta_\varepsilon}{2}\sigma_Z + \hbar\omega_0(a^+a + 1/2) + H_{int} \quad (3)$$

where $\Delta_\varepsilon = \sqrt{\Delta^2 + \varepsilon^2}$ is the gap between two energy states and

$$H_{int} = \left(\frac{\Delta}{\Delta_\varepsilon}\sigma_X - \frac{\varepsilon}{\Delta_\varepsilon}\sigma_Z\right)F(a^+ + a) \quad (4)$$

First we consider noninteracting system TLS+ laser field which is described by Hamiltonian:

$$H_0 = \frac{\Delta_\varepsilon}{2}\sigma_Z + \hbar\omega_0(a^+a + 1/2) \quad (5)$$

We denote as $|a\rangle$ and $|b\rangle$ the ground state and excited state wave functions of TLS, respectively with the properties: $\sigma_Z|a\rangle = -|a\rangle$, $\sigma_Z|b\rangle = |b\rangle$, $\sigma_X|a\rangle = |b\rangle$, $\sigma_X|b\rangle = |a\rangle$. The eigenfunctions of the photon field are $|N\rangle$: $a^+|N\rangle = \sqrt{N+1}|N+1\rangle$, $a|N\rangle = \sqrt{N}|N-1\rangle$. The eigenfunctions of the noninteracting TLS+photon system we denote as a tensor product $|a, N\rangle \equiv |a\rangle \otimes |N\rangle$, $|b, N\rangle \equiv |b\rangle \otimes |N\rangle$. Up to a constant term the energies of these states are:

$$H_0|a, N\rangle = -\frac{\Delta_\varepsilon}{2} + \hbar\omega_0 N \quad (6)$$

$$H_0|b, N\rangle = \frac{\Delta_\varepsilon}{2} + \hbar\omega_0 N \quad (7)$$

Let the photon frequency ω_0 is close to the TLS frequency $\Delta_\varepsilon/\hbar$ with a small detuning $\delta = \omega_0 - \Delta_\varepsilon/\hbar \ll \omega_0, \Delta_\varepsilon/\hbar$, where for definitiveness we assume $\delta > 0$. Then it is seen from (6) and (7) that the energies of the states $|a, N+1\rangle$ and $|b, N\rangle$ are close to each other: $E_{a,N+1} - E_{b,N} = \hbar\delta$. The same is true for the pairs of states $|a, N\rangle$ and $|b, N-1\rangle$; $|a, N+2\rangle$ and $|b, N+1\rangle$, and so on. Therefore, the energy levels of noninteracting system TLS+photon field is a ladder of manifolds (see Fig. 1).

Every manyfold is parameterized by a pair of states with a small spacing between them, $\hbar\delta$, and the distance between neighbor manifolds is equal to photon energy, $\hbar\omega_0$.

This ladder of manifolds is quite similar to the one for atom-field interaction[19]. However, a principal difference is the structure of interaction Hamiltonian (4). In quantum optics there is no "longitudinal" interaction between atom spin and a photon field which is proportional to σ_Z. It is the presence of this bias interaction in dissipative TLS that leads to some effects which are unobservable in quantum optics.

Consider now the modification of these levels that results from the interaction (4). We take a pair of the closed spacing levels within a given manifold, $|a, N\rangle$, $|b, N-1\rangle$. The interaction (4) causes a transition between these levels with the amplitude

$$\langle a, N|H_{int}|b, N-1\rangle = \frac{\Delta F}{2\Delta_\varepsilon}\sqrt{N} \quad (8)$$

In addition, the interaction (4) connects the level $|a, N\rangle$ to the levels of the neighbor manifolds, $|b, N+1\rangle$, $|a, N+1\rangle$, $|a, N-1\rangle$,. In the same way the level $|b, N-1\rangle$ is additionally connected to $|a, N-2\rangle$, $|b, N\rangle$, $|b, N-2\rangle$. Therefore, the wave functions of the levels $|a, N\rangle$ and $|b, N-1\rangle$ are modified as follows:

$|a, N+2\rangle$

$|b, N+1\rangle$

$\hbar\delta$

$|a, N+1\rangle$

$|b, N\rangle$

$\hbar\omega_0$

$|a, N\rangle$

$|b, N-1\rangle$

$|a, N-1\rangle$
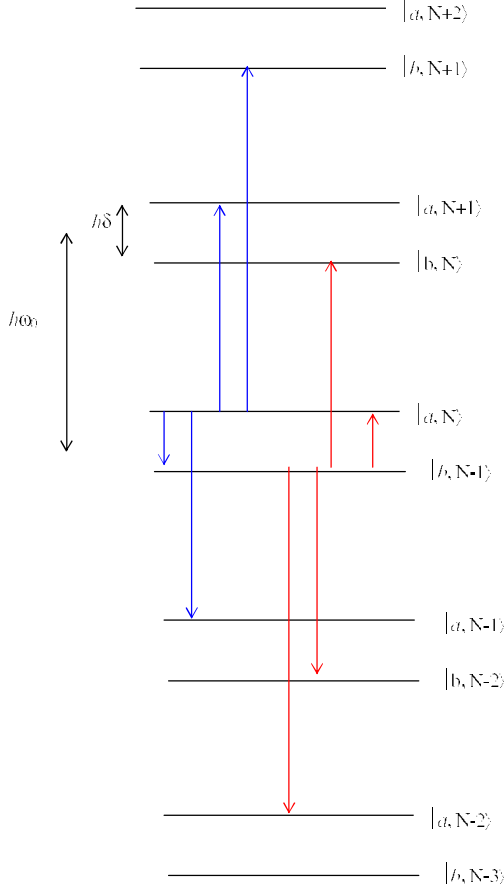
$|b, N-2\rangle$

$|a, N-2\rangle$

$|b, N-3\rangle$

FIG. 1: (Color online). Levels of noninteracting TLS+photon field system. The level spacing in a given manifold is $\hbar\delta$. The spacing between neighbor manifolds is $\hbar\omega_0$. The red (blue) arrows shows the H_{int} induced transitions from the state $|b, N-1\rangle$ ($|a, N\rangle$).

$$|a, N\rangle \rightarrow |1, N\rangle = A_1|a, N\rangle + B_1|b, N-1\rangle +$$
$$C_1|b, N+1\rangle + D_1|a, N+1\rangle + E_1|a, N-1\rangle \quad (9)$$

$$|b, N-1\rangle \rightarrow |2, N\rangle = A_2|a, N\rangle + B_2|b, N-1\rangle +$$
$$C_2|a, N-2\rangle + D_2|b, N\rangle + E_2|b, N-2\rangle \quad (10)$$

where we define the state with higher energy as $|1, N\rangle$.

The quantities C_1 and C_2 are due to the "transversal" part of the interaction Hamiltonian, which is proportional to σ_X, while the quantities D_1, E_1, D_2, and E_2 are due to its "longitudinal part" which is proportional to σ_Z. All these quantities describe transition to neighbor manifolds, therefore they are on the order of F/ω_0. It is worth noting that the last two terms in (9) and (10) are peculiar to TLS and are absent in quantum

optics. In what follows we assume a weak excitation amplitude ($F/\omega_0 \ll 1$), therefore we leave in Eqs. (9), (10) only first two terms in their right hand sides:

$$|1, N\rangle = \sin\theta|a, N\rangle + \cos\theta|b, N-1\rangle \quad (11)$$

$$|2, N\rangle = -\cos\theta|a, N\rangle + \sin\theta|b, N-1\rangle \quad (12)$$

The form of Eqs. (11) and (12) insures the normalization and orthogonality of wave functions $|1, N\rangle$ and $|2, N\rangle$, which are eigenfunctions of Hamiltonian (3). Accordingly, the uncoupled states $|a, N\rangle$, $|b, N-1\rangle$ can be expressed in terms of dressed states $|1, N\rangle$, $|2, N\rangle$:

$$|a, N\rangle = \sin\theta|1, N\rangle - \cos\theta|2, N\rangle \quad (13)$$

$$|b, N-1\rangle = \cos\theta|1, N\rangle + \sin\theta|2, N\rangle \quad (14)$$

By using the standard quantum mechanical technique we find eigenenergies and the angle θ:

$$E_{\pm} = \frac{1}{2}\left(E_{|a,N\rangle} + E_{|b,N-1\rangle}\right) \pm \frac{1}{2}\hbar\Omega_R \quad (15)$$

where upper (lower) sign corresponds to $|1, N\rangle$ ($|2, N\rangle$). The quantity Ω_R in (15) is the Rabi frequency[21]

$$\Omega_R = \sqrt{\delta^2 + \Omega_1^2} \quad (16)$$

where $\Omega_1 = \Delta F/\Delta_\varepsilon$, and we incorporated $\sqrt{N}$ in the high frequency amplitude F.

For the angle θ we obtain $\tan 2\theta = -\Omega_1/\delta$, where $0 < 2\theta < \pi$, so that $\cos 2\theta = -\delta/\Omega_R$, $\cos\theta = \frac{1}{\sqrt{2}}\left(1 - \frac{\delta}{\Omega_R}\right)^{1/2}$, $\sin\theta = \frac{1}{\sqrt{2}}\left(1 + \frac{\delta}{\Omega_R}\right)^{1/2}$.

When the interaction is switched off ($F \rightarrow 0$) then, as should be expected, the state $|1, N\rangle$ tends to $|a, N\rangle$, and the state $|2, N\rangle$ tends to $|b, N-1\rangle$.

Therefore, with account for the interaction between TLS and the photon field the level structure of a given manifold looks like that shown in Fig. 2. The interaction increases the energy gap between the states $|a, N\rangle$ and $|b, N-1\rangle$. They say these states are dressed by the interaction. In what follows we call these two nearby dressed states as Rabi levels.

Up to now the picture is quite similar to that known from atom-photon interaction[19]. However, a drastic difference appears if we consider the excitation of the dressed levels $|1, N\rangle$ and $|2, N\rangle$ by a signal whose frequency is compared with Rabi frequency Ω_R. Such a low frequency signal cannot change the number N of high frequency photons, therefore, in quantum optics the transition between these two states are not allowed since the atom dipole operator connects only the levels, say $|a, N\rangle$ and $|b, N\rangle$, which belong to the different manifolds. In our language, the atom dipole operator is transversal: it is proportional to σ_X.
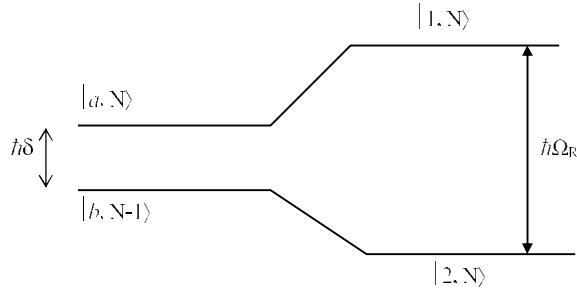
3

FIG. 2: The level structure of a dressed manifold. The uncoupled states $|a, N\rangle$ and $|b, N - 1\rangle$ are converted by the interaction between TLS and photon field into the two dressed states $|1, N\rangle$ and $|2, N\rangle$.

In TLS the transitions between states $|1, N\rangle$ and $|2, N\rangle$ are caused by "longitudinal" term in interaction Hamiltonian, which is proportional to σ_Z. Let us assume the system (1) additionally interacts with a low frequency signal $G \cos \omega t$, so that Hamiltonian (1) is added by the term $-\sigma_z G \cos \omega t$, where the frequency ω is on the order of Rabi frequency Ω_R. In eigenbasis this low frequency Hamiltonian is transformed as follows:

$$H_{int}^{LF} = \left(\frac{\Delta}{\Delta_\varepsilon} \sigma_X - \frac{\varepsilon}{\Delta_\varepsilon} \sigma_Z \right) G \cos \omega t \qquad (17)$$

The transitions between the Rabi levels $|1, N\rangle$ and $|2, N\rangle$ are caused by the second term in brackets of (17):

$$\langle 1, N | H_{int}^{LF} | 2, N \rangle = -\frac{\varepsilon G \Omega_1}{\Delta_\varepsilon \Omega_R} \qquad (18)$$

In what follows we show that these transitions result in the undamped low frequency oscillations of the populations of initial levels $|a\rangle$ and $|b\rangle$ which can be detected by a corresponding electronic circuitry.

III. RATE EQUATIONS FOR THE DENSITY MATRIX IN UNCOUPLED BASIS

The elements of density matrix σ in the basis of uncoupled levels $|a, N\rangle$ and $|b, N\rangle$ are defined as follows:

$$\begin{aligned} \sigma_{aa} &= \langle a, N | \sigma | a, N \rangle \\ \sigma_{bb} &= \langle b, N | \sigma | b, N \rangle \qquad (19) \\ \sigma_{ab} &= \langle a, N | \sigma | b, N - 1 \rangle \end{aligned}$$

The rate equations for the density matrix σ can be written in the following form:

$$\frac{d\sigma_{bb}}{dt} = -\sigma_{bb} \Gamma_\downarrow + \sigma_{aa} \Gamma_\uparrow \qquad (20)$$

$$\frac{d\sigma_{aa}}{dt} = -\sigma_{aa} \Gamma_\uparrow + \sigma_{bb} \Gamma_\downarrow \qquad (21)$$

$$\frac{d\sigma_{ab}}{dt} = i \delta \sigma_{ab} - \sigma_{ab} \Gamma_\varphi \qquad (22)$$

where $\Gamma_\downarrow$ is the transition rate from the state $|b, N\rangle$ to state $|a, N\rangle$ (relaxation rate), $\Gamma_\uparrow$ is the transition rate from the state $|a, N\rangle$ to state $|b, N\rangle$ (excitation rate), the quantity Γ_φ is the rate of decoherence. These three equations can be written in the operator form:

$$\frac{d\sigma}{dt} = -\frac{i}{\hbar} [H_0, \sigma] + \widehat{L} \qquad (23)$$

where Hamiltonian of the uncoupled system H_0 is given in (5). The operator $\widehat{L}$ is defined by its matrix elements which follows from (20), (21) and (22):

$$\langle b, N | \widehat{L} | b, N \rangle = -\sigma_{bb} \Gamma_\downarrow + \sigma_{aa} \Gamma_\uparrow \qquad (24)$$

$$\langle a, N | \widehat{L} | a, N \rangle = -\sigma_{aa} \Gamma_\uparrow + \sigma_{bb} \Gamma_\downarrow \qquad (25)$$

$$\langle a, N | \widehat{L} | b, N - 1 \rangle = -\sigma_{ab} \Gamma_\varphi \qquad (26)$$

IV. RATE EQUATIONS FOR THE DENSITY MATRIX IN THE BASIS OF RABI LEVELS $|1, N\rangle$ AND $|2, N\rangle$

The equation (23) can be generalized to include the interaction between TLS and laser field:

$$\frac{d\sigma}{dt} = -\frac{i}{\hbar} [H, \sigma] + \widehat{L} \qquad (27)$$

where Hamiltonian H is given in (3) with H_{int} from (4). Since the equation (27) is valid in any basis we can find the elements of density matrix σ over the basis of dressed states:

$$\frac{d\langle 1, N | \sigma | 1, N \rangle}{dt} = \langle 1, N | \widehat{L} | 1, N \rangle \qquad (28)$$

$$\frac{d\langle 2, N | \sigma | 2, N \rangle}{dt} = \langle 2, N | \widehat{L} | 2, N \rangle \qquad (29)$$

$$\frac{d\langle 1, N | \sigma | 2, N \rangle}{dt} = -i\Omega_R \langle 1, N | \sigma | 2, N \rangle + \langle 1, N | \widehat{L} | 2, N \rangle \qquad (30)$$

Below we define the reduced density matrix for two level coupled system by tracing over the photon number N:

$$\rho_{11} = \sum_N \langle 1, N | \sigma | 1, N \rangle$$

$$\rho_{22} = \sum_N \langle 2, N | \sigma | 2, N \rangle$$

$$\rho_{12} = \sum_N \langle 1, N | \sigma | 2, N \rangle$$

$$\rho_{21} = \sum_N \langle 2, N | \sigma | 1, N \rangle \qquad (31)$$

Taking into account the matrix elements of $\widehat{L}$ in the dressed state basis, calculated in Appendix A, we obtain the rate equations for the reduced density matrix ρ. The rate equations for diagonal elements of ρ are as follows:

$$\frac{d\rho_{11}}{dt} = -\Gamma_1\rho_{11} + \Gamma_2\rho_{22} + \Gamma_0(\rho_{12} + \rho_{21}) \quad (32)$$

$$\frac{d\rho_{22}}{dt} = -\Gamma_2\rho_{22} + \Gamma_1\rho_{11} - \Gamma_0(\rho_{12} + \rho_{21}) \quad (33)$$

where

$$\Gamma_1 = \left[\cos 2\theta \left(\Gamma_\downarrow \cos^2\theta - \Gamma_\uparrow \sin^2\theta\right) + 2\Gamma_\varphi \sin^2\theta\cos^2\theta\right] \quad (34)$$

$$\Gamma_2 = \left[\cos 2\theta \left(\Gamma_\uparrow \cos^2\theta - \Gamma_\downarrow \sin^2\theta\right) + 2\Gamma_\varphi \sin^2\theta\cos^2\theta\right] \quad (35)$$

$$\Gamma_0 = \sin\theta\cos\theta\cos 2\theta\left[\Gamma_\varphi - \Gamma_\uparrow - \Gamma_\downarrow\right] \quad (36)$$

As is seen from (32) and (33), the total population is constant: $\frac{d}{dt}(\rho_{11}+\rho_{22}) = 0$. In our case the normalization condition is $\rho_{11} + \rho_{22} = 1$.

For off diagonal elements of ρ we obtain the rate equations:

$$\frac{d\rho_{12}}{dt} = -i\Omega_R\rho_{12}+$$
$$\rho_{11}\sin\theta\cos\theta\left[2\Gamma_\uparrow sin^2\theta - 2\Gamma_\downarrow\cos^2\theta + \Gamma_\varphi cos2\theta\right]+$$
$$\rho_{22}\sin\theta\cos\theta\left[2\Gamma_\uparrow cos^2\theta - 2\Gamma_\downarrow\sin^2\theta - \Gamma_\varphi cos2\theta\right]-$$
$$\rho_{12}\left[2\sin^2\theta\cos^2\theta\left(\Gamma_\uparrow + \Gamma_\downarrow\right) + \Gamma_\varphi\left(cos^4\theta + sin^4\theta\right)\right]-$$
$$\rho_{21}2\sin^2\theta\cos^2\theta\left[\Gamma_\uparrow + \Gamma_\downarrow - \Gamma_\varphi\right]+ \quad (37)$$

Since $\rho_{12} = \rho_{21}^\dagger$, the rate equation for ρ_{21} is obtained from (37) by hermitian conjugate.

V. BLOCH TYPE EQUATIONS FOR THE DENSITY MATRIX

The rate equations can be further simplified if we introduce new variables: $\rho = \rho_{11} - \rho_{22}$, $\rho_+ = \rho_{12} + \rho_{21}$, $\rho_- = \rho_{12} - \rho_{21}$. The rate equations for ρ, ρ_+, ρ_- are as follows:

$$\frac{d\rho}{dt} = -\rho\left[\frac{1}{T_1}\cos^2 2\theta + \Gamma_\varphi\sin^2 2\theta\right]+$$
$$\rho_+\left[\Gamma_\varphi - \frac{1}{T_1}\right]\sin 2\theta\cos 2\theta + \Gamma_-\cos 2\theta \quad (38)$$

$$\frac{d\rho_+}{dt} = -i\Omega_R\rho_- + \rho\left[\Gamma_\varphi - \frac{1}{T_1}\right]\sin 2\theta\cos 2\theta-$$
$$\rho_+\left[\frac{1}{T_1}\sin^2 2\theta - \Gamma_\varphi\cos^2 2\theta\right] + \Gamma_-\sin 2\theta \quad (39)$$

$$\frac{d\rho_-}{dt} = -i\Omega_R\rho_+ - \Gamma_\varphi\rho_- \quad (40)$$

where $\frac{1}{T_1} = \Gamma_\uparrow + \Gamma_\downarrow$, $\Gamma_- = \Gamma_\uparrow - \Gamma_\downarrow$.

If the damping is absent (all Γ's in (38), (39), (40) are equal to zero) the quantity ρ is constant and ρ_+, ρ_- oscillate with the Rabi frequency Ω_R. However, in the presence of a damping these oscillations rapidly decay to give the steady state solutions of Eqs. (38), (39), (40)(see Appendix B).

Here it is instructive to consider the case when the high frequency detuning δ is small compared to the Rabi frequency at zero detuning ($\delta \ll \Omega_1$). In this limit $\sin 2\theta \to 1$, $\cos 2\theta \to -\delta/\Omega_1$ and we get from the Eqs. (38), (39), (40):

$$\frac{d\rho}{dt} = -\Gamma_\varphi\rho \quad (41)$$

$$\frac{d\rho_+}{dt} = -i\Omega_1\rho_- - \frac{1}{T_1}\rho_+ + \Gamma_- \quad (42)$$

$$\frac{d\rho_-}{dt} = -i\Omega_1\rho_+ - \Gamma_\varphi\rho_- \quad (43)$$

It is seen that the population ρ decays with the decoherence rate Γ_φ. This is due to the fact that in the dressed state model the population of the level, say, $|1,N\rangle$ can only be changed as a result of spontaneous transitions to the levels $|1,N-1\rangle$ and $|2,N-1\rangle$ of the neighbor manifold. The offdiagonal quantities ρ_+, ρ_- undergo the damping oscillation with the rate $\frac{1}{2}\left(\frac{1}{T_1} + \Gamma_\varphi\right)$ provided that $\Omega_1 > \frac{1}{2}\left(\frac{1}{T_1} - \Gamma_\varphi\right)$. The nonzero steady state solution of Eq. (38) for small detuning ($\delta \ll \Omega_1$), and those for (42), (43) for $\delta = 0$ are as follows:

$$\rho^{(0)} = -\frac{\delta}{\Gamma_\varphi\Omega_1}\frac{\Gamma_-\left(\Gamma_\varphi^2 + \Omega_1^2\right)}{\Omega_1^2 + \frac{\Gamma_\varphi}{T_1}} \quad (44)$$

$$\rho_+^{(0)} = \frac{\Gamma_-\Gamma_\varphi}{\Omega_1^2 + \frac{\Gamma_\varphi}{T_1}} \quad (45)$$

$$\rho_-^{(0)} = -i\frac{\Gamma_-\Omega_1}{\Omega_1^2 + \frac{\Gamma_\varphi}{T_1}} \quad (46)$$

As is seen from (44) $\rho^{(0)} \to 0$ as δ tends to zero that means the equalization of the population of two levels ($\rho_{11} = \rho_{22} = \frac{1}{2}$).

VI. EXCITATION OF RABI LEVELS BY A LOW FREQUENCY SIGNAL

Here we find the response of the coupled TLS+photon system to the external signal the frequency of which is of the order of Rabi frequency Ω_R. The operator equation for the density matrix σ is similar to (27):

$$\frac{d\sigma}{dt} = -\frac{i}{\hbar}[H + H_{int}^{LF}, \sigma] + \widehat{L} \qquad (47)$$

where Hamiltonian H_{int}^{LF} is given in (17).

Since the low frequency signal cannot change the photon number N, the transitions between Rabi levels $|1, N\rangle$ and $|2.N\rangle$ can be induced only by the second term in low frequency Hamiltonian (17). The equations for ρ, ρ_+ and ρ_- are obtained in the same way as Eqs. (38), (39), (40). The only difference is appearance of low frequency terms in right hand sides of (38), (39), (40). Therefore, taking into account the low frequency excitation, we get for the reduced density matrix the following Bloch like equations:

$$\frac{d\rho}{dt} = -\rho \left[\frac{1}{T_1}\cos^2 2\theta + \Gamma_\varphi \sin^2 2\theta\right] +$$
$$\rho_+ \left[\Gamma_\varphi - \frac{1}{T_1}\right] \sin 2\theta \cos 2\theta +$$
$$\rho_- (ig \sin 2\theta \cos \omega t) + \Gamma_- \cos 2\theta \qquad (48)$$

$$\frac{d\rho_+}{dt} = -i\Omega_R \rho_- + \rho \left[\Gamma_\varphi - \frac{1}{T_1}\right] \sin 2\theta \cos 2\theta -$$
$$\rho_+ \left[\frac{1}{T_1}\sin^2 2\theta - \Gamma_\varphi \cos^2 2\theta\right] +$$
$$\rho_- (ig \cos 2\theta \cos \omega t) + \Gamma_- \sin 2\theta \qquad (49)$$

$$\frac{d\rho_-}{dt} = -i\Omega_R \rho_+ - \Gamma_\varphi \rho_- + ig (\rho_+ \cos 2\theta - \rho \sin 2\theta) \cos \omega t \qquad (50)$$

where $g = 2\varepsilon G/\Delta_\varepsilon$.

It is evident that the above equations exhibit oscillation solutions in presence of the damping. If the excitation amplitude is rather small we may obtain the time dependent solutions of (48), (49), (50) as the small time dependent corrections to steady state values, which are given in Appendix B: $\rho(t) = \rho^{(0)} + \rho^{(1)}(t)$, $\rho_+(t) = \rho_+^{(0)} + \rho_+^{(1)}(t)$, $\rho_-(t) = \rho_-^{(0)} + \rho_-^{(1)}(t)$.

The equations for these time dependent corrections are as follows:

$$\frac{d\rho^{(1)}}{dt} = -\rho^{(1)} \left[\frac{1}{T_1}\cos^2 2\theta + \Gamma_\varphi \sin^2 2\theta\right] +$$
$$\rho_+^{(1)} \left[\Gamma_\varphi - \frac{1}{T_1}\right] \sin 2\theta \cos 2\theta +$$
$$\rho_-^{(0)} (ig \sin 2\theta \cos \omega t) \qquad (51)$$

$$\frac{d\rho_+^{(1)}}{dt} = -i\Omega_R \rho_-^{(1)} + \rho^{(1)} \left[\Gamma_\varphi - \frac{1}{T_1}\right] \sin 2\theta \cos 2\theta -$$
$$\rho_+^{(1)} \left[\frac{1}{T_1}\sin^2 2\theta - \Gamma_\varphi \cos^2 2\theta\right] +$$
$$\rho_-^{(0)} (ig \cos 2\theta \cos \omega t) \qquad (52)$$

$$\frac{d\rho_-^{(1)}}{dt} = -i\Omega_R \rho_+^{(1)} - \Gamma_\varphi \rho_-^{(1)} +$$
$$ig \left(\rho_+^{(0)} \cos 2\theta - \rho^{(0)} \sin 2\theta\right) \cos \omega t \qquad (53)$$

From these equations it is not difficult to find the linear susceptibilities of the system $(\chi_\rho(\omega) = \rho(\omega)/G$, etc.$)$:

$$\chi_\rho(\omega) = \frac{2\varepsilon\Omega_R}{D(\omega)\Gamma_\varphi\Delta_\varepsilon} \left[\rho_+^{(0)} \left[(i\omega + \Gamma_\varphi)\left[(i\omega + A_2)\sin 2\theta + B\cos 2\theta\right] + B\Gamma_\varphi \cos 2\theta + \Omega_R^2 \sin 2\theta\right] - B\Omega_R \rho^{(0)} \sin 2\theta\right] \qquad (54)$$

$$\chi_{\rho+}(\omega) = \frac{2\varepsilon\Omega_R}{D(\omega)\Gamma_\varphi\Delta_\varepsilon} \left[\rho_+^{(0)} \left[(i\omega + A_1)(i\omega + 2\Gamma_\varphi)\cos 2\theta + B(i\omega + \Gamma_\varphi)\sin 2\theta\right] - (i\omega + A_1)\Gamma_\varphi \rho^{(0)} \sin 2\theta\right] \qquad (55)$$

$$\chi_{\rho_-}(\omega) = i\frac{2\varepsilon\Omega_R}{D(\omega)\Gamma_\varphi\Delta_\varepsilon}\times$$

$$\left[\frac{\Gamma_\varphi}{\Omega_R}\left[(i\omega+A_1)\left(i\omega+A_2\right)-B^2\right]\left(\rho_+^{(0)}\cos2\theta-\rho^{(0)}\sin2\theta\right)-\rho_+^{(0)}\Omega_R\left[B\sin2\theta+(i\omega+A_1)\cos2\theta\right]\right] \quad (56)$$

where

$$D(\omega)=(i\omega+\Gamma_\varphi)\left[(i\omega+A_1)\left(i\omega+A_2\right)-B^2\right]+\Omega_R^2\left(i\omega+A_1\right) \quad (57)$$

In principle, the Eqs. (54), (55), (56) solve our problem: they give a response of the coupled system TLS+photon field to a low frequency signal, which excites transitions between the Rabi levels.

A. Small high frequency detuning

If the high frequency detuning δ is small compared with the zero detuning Rabi frequency Ω_1 ($\delta \ll \Omega_1$), the Eqs. (51), (52), (53) can be substantially simplified. In the limit $\delta = 0$ for Eq. (51) we get:

$$\frac{d\rho^{(1)}}{dt}+\Gamma_\varphi\rho^{(1)}=ig\rho_-^{(0)}\cos\omega t \quad (58)$$

Therefore, at exact resonance the quantity $\rho^{(1)}$ oscillates without damping. However, in order to obtain oscillatory behavior for $\rho_+^{(1)}$ and $\rho_-^{(1)}$ we have to keep in right hand sides of (52), (53) the terms which are linear in δ. Thus, in the limit of small δ we get from (52), (53):

$$\frac{d\rho_+^{(1)}}{dt}+i\Omega_1\rho_-^{(1)}+\frac{1}{T_1}\rho_+^{(1)}=$$
$$-ig\frac{\delta}{\Omega_1}\rho_-^{(0)}\cos\omega t-\frac{\delta}{\Omega_1}\left(\Gamma_\varphi-\frac{1}{T_1}\right)\rho^{(1)} \quad (59)$$

$$\frac{d\rho_-^{(1)}}{dt}+i\Omega_1\rho_+^{(1)}+\Gamma_\varphi\rho_-^{(1)}=-ig\left(\frac{\delta}{\Omega_1}\rho_+^{(0)}+\rho^{(0)}\right)\cos\omega t \quad (60)$$

The quantity $\rho^{(1)}$ in (59) is the solution of (58), which does not depend on δ.

From the Eqs. (58), (59), (60) we find the linear susceptibilities of the coupled system TLS+photon field for the case of small high frequency detuning:

$$\chi_\rho(\omega)=\frac{2\varepsilon}{\Delta_\varepsilon}\frac{i\rho_-^{(0)}}{i\omega+\Gamma_\varphi} \quad (61)$$

$$\chi_{\rho_+}(\omega)=\frac{2\varepsilon}{\Delta_\varepsilon}\frac{i\delta\rho_-^{(0)}}{\Omega_1 d(\omega)}\left[\frac{\Omega_1^2}{\Gamma_\varphi}-i\omega-2\Gamma_\varphi+\frac{1}{T_1}\right] \quad (62)$$

$$\chi_{\rho_-}(\omega)=-\frac{2\varepsilon}{\Delta_\varepsilon}\frac{\delta\rho_-^{(0)}}{\Omega_1\Gamma_\varphi\left(i\omega+\Gamma_\varphi\right)d(\omega)}\times$$
$$\left[\left(i\omega+\frac{1}{T_1}\right)\left(i\omega+\Gamma_\varphi\right)+\Gamma_\varphi\left(i\omega+2\Gamma_\varphi-\frac{1}{T_1}\right)\right] \quad (63)$$

where

$$d(\omega)=\left(i\omega+\frac{1}{T_1}\right)\left(i\omega+\Gamma_\varphi\right)+\Omega_1^2 \quad (64)$$

The resonance nature of the response is evident from (64).

B. Measurable quantities

Any quantity measurable in low frequency domain can be expressed as a trace within a given manifold over the photon numbers N. For example:

$$\langle\sigma_Z\rangle=Tr\left(\sigma\sigma_Z\right)=$$
$$\sum_N\langle1,N|\sigma\sigma_Z|1,N\rangle+\sum_N\langle2,N|\sigma\sigma_Z|2,N\rangle=$$
$$\sum_N\langle1,N|\sigma|1,N\rangle\langle1,N|\sigma_Z|1,N\rangle+$$
$$\sum_N\langle1,N|\sigma|2,N\rangle\langle2,N|\sigma_Z|1,N\rangle+$$
$$\sum_N\langle2,N|\sigma|1,N\rangle\langle1,N|\sigma_Z|2,N\rangle+$$
$$\sum_N\langle2,N|\sigma|2,N\rangle\langle2,N|\sigma_Z|2,N\rangle=$$
$$\rho\cos2\theta+\rho_+\sin2\theta \quad (65)$$

where we have used the definitions of density matrix (31) and the dressed states (11), (12). The same result (Eq. (65)) we would get if we took the trace over uncoupled basis $|a,N\rangle$, $|b,N\rangle$.

For small amplitude G of low frequency excitation we therefore, get:

$$\langle\sigma_Z\rangle=\rho^{(0)}\cos2\theta+\rho_+^{(0)}\sin2\theta+\rho^{(1)}(t)\cos2\theta+\rho_+^{(1)}(t)\sin2\theta \quad (66)$$

where $\rho^{(1)}(t)$ and $\rho_+^{(1)}(t)$ can be expressed in terms of real (χ') and imaginary (χ'') parts of their corresponding susceptibilities: $\rho^{(1)}(t) = G\left(\chi'_\rho \cos\omega t - \chi''_\rho \sin\omega t\right)$, $\rho_+^{(1)}(t) = G\left(\chi'_{\rho_+} \cos\omega t - \chi''_{\rho_+} \sin\omega t\right)$.

In the same way we get:

$$\langle \frac{d\sigma_Z}{dt} \rangle = Tr\left(-\frac{i}{\hbar}[H,\sigma_Z]\sigma\right) = i\Omega_R \sin 2\theta \rho_-(t) \quad (67)$$

For small amplitude G

$$\langle \frac{d\sigma_Z}{dt} \rangle = i\Omega_R \sin 2\theta \rho_-^{(0)} + i\Omega_R \sin 2\theta \rho_-^{(1)}(t) \quad (68)$$

where $\rho_-^{(1)}(t) = G\left(\chi'_{\rho_-} \cos\omega t - \chi''_{\rho_-} \sin\omega t\right)$.

As for the quantities σ_X and σ_Y, it is not difficult to show that $\langle\sigma_X\rangle = 0$, and $\langle\sigma_Y\rangle = 0$ when averaging over N within a given manifold. It means the absence of the low frequency oscillations for these quantities[22].

VII. CONCLUSION

In this paper in the frame of the dressed state approach we have analyzed the interaction of a dissipative two level quantum system with high and low frequency excitations. We have found the response of the coupled TLS+photon

field system to a signal whose frequency is on the order of the Rabi frequency. In this case the response of the system exhibits an undamped low frequency oscillations, whose amplitude has a clear resonance at the Rabi frequency with the width being dependent on the damping rates of the system. The method can be useful for low-frequency Rabi spectroscopy in various physical systems which are described by a two-level Hamiltonian, such as nuclei spins in NMR, double well quantum dots, superconducting flux and charge qubits, etc.

VIII. APPENDIX

A. Calculation of matrix elements of $\widehat{L}$ in dressed state basis

With the aid of (11), (12) and (24), (25), (26) we obtain for $\langle 1,N|\widehat{L}|1,N\rangle$:

$$\langle 1,N|\widehat{L}|1,N\rangle =$$
$$\sin^2\theta\langle a,N|\widehat{L}|a,N\rangle + \cos^2\theta\langle b,N-1|\widehat{L}|b,N-1\rangle + \sin\theta\cos\theta\left[\langle a,N|\widehat{L}|b,N-1\rangle + \langle b,N-1|\widehat{L}|a,N\rangle\right] =$$
$$\sin^2\theta\left[-\Gamma_\uparrow\langle a,N|\sigma|a,N\rangle + \Gamma_\downarrow\langle b,N|\sigma|b,N\rangle\right] + \cos^2\theta\left[-\Gamma_\downarrow\langle b,N-1|\sigma|b,N-1\rangle + \Gamma_\uparrow\langle a,N-1|\sigma|a,N-1\rangle\right] -$$
$$\Gamma_\varphi\sin\theta\cos\theta\left[\langle a,N|\sigma|b,N-1\rangle + \langle b,N-1|\sigma|a,N\rangle\right] \quad (69)$$

Further transformation requires the substitution of uncoupled states in (69) with the dressed states by using Eqs. (13), (14). As a result we obtain:

$$\langle 1,N|\widehat{L}|1,N\rangle =$$
$$-\langle 1,N|\sigma|1,N\rangle\left[\Gamma_\uparrow\sin^4\theta + \Gamma_\downarrow\cos^4\theta + 2\Gamma_\varphi\sin^2\theta\cos^2\theta\right] - \langle 2,N|\sigma|2,N\rangle\sin^2\theta\cos^2\theta\left[\Gamma_\uparrow + \Gamma_\downarrow - 2\Gamma_\varphi\right] +$$
$$\left[\langle 1,N|\sigma|2,N\rangle + \langle 2,N|\sigma|1,N\rangle\right]\sin\theta\cos\theta\left[\Gamma_\uparrow\sin^2\theta - \Gamma_\downarrow\cos^2\theta + \Gamma_\varphi\cos 2\theta\right] + \sin^2\theta\cos^2\theta\Gamma_\downarrow\langle 1,N+1|\sigma|1,N+1\rangle +$$
$$\sin^2\theta\cos^2\theta\Gamma_\uparrow\langle 1,N-1|\sigma|1,N-1\rangle + \sin^4\theta\Gamma_\downarrow\langle 2,N+1|\sigma|2,N+1\rangle + \cos^4\theta\Gamma_\uparrow\langle 2,N-1|\sigma|2,N-1\rangle +$$
$$\left[\langle 1,N+1|\sigma|2,N+1\rangle + \langle 2,N+1|\sigma|1,N+1\rangle\right]\Gamma_\downarrow\sin^3\theta\cos\theta -$$
$$\left[\langle 1,N-1|\sigma|2,N-1\rangle + \langle 2,N-1|\sigma|1,N-1\rangle\right]\Gamma_\uparrow\sin\theta\cos^3\theta \quad (70)$$

By doing the same transformations we obtain:

$$\langle 2,N|\widehat{L}|2,N\rangle =$$
$$- \langle 2,N|\sigma|2,N\rangle \left[\Gamma_\uparrow \cos^4\theta + \Gamma_\downarrow \sin^4\theta + 2\Gamma_\varphi \sin^2\theta \cos^2\theta\right] - \langle 1,N|\sigma|1,N\rangle \sin^2\theta \cos^2\theta \left[\Gamma_\uparrow + \Gamma_\downarrow - 2\Gamma_\varphi\right] +$$
$$\left[\langle 1,N|\sigma|2,N\rangle + \langle 2,N|\sigma|1,N\rangle\right] \sin\theta \cos\theta \left[\Gamma_\uparrow \cos^2\theta - \Gamma_\downarrow \sin^2\theta - \Gamma_\varphi \cos 2\theta\right] + \sin^2\theta \cos^2\theta \Gamma_\downarrow \langle 2,N+1|\sigma|2,N+1\rangle +$$
$$\sin^2\theta \cos^2\theta \Gamma_\uparrow \langle 2,N-1|\sigma|2,N-1\rangle + \cos^4\theta \Gamma_\downarrow \langle 1,N+1|\sigma|1,N+1\rangle + \sin^4\theta \Gamma_\uparrow \langle 1,N-1|\sigma|1,N-1\rangle +$$
$$\left[\langle 1,N+1|\sigma|2,N+1\rangle + \langle 2,N+1|\sigma|1,N+1\rangle\right] \Gamma_\downarrow \cos^3\theta \sin\theta -$$
$$\left[\langle 1,N-1|\sigma|2,N-1\rangle + \langle 2,N-1|\sigma|1,N-1\rangle\right] \Gamma_\uparrow \sin^3\theta \cos\theta \quad (71)$$

$$\langle 1,N|\widehat{L}|2,N\rangle =$$
$$\langle 1,N|\sigma|1,N\rangle \sin\theta \cos\theta \left[\Gamma_\uparrow \sin^2\theta - \Gamma_\downarrow \cos^2\theta + \Gamma_\varphi \cos 2\theta\right] + \langle 2,N|\sigma|2,N\rangle \sin\theta \cos\theta \left[\Gamma_\uparrow \cos^2\theta - \Gamma_\downarrow \sin^2\theta - \Gamma_\varphi \cos 2\theta\right] -$$
$$\langle 1,N|\sigma|2,N\rangle \left[(\Gamma_\uparrow + \Gamma_\downarrow)\cos^2\theta \sin^2\theta + \Gamma_\varphi \left(\cos^4\theta + \sin^4\theta\right)\right] - \langle 2,N|\sigma|1,N\rangle \sin^2\theta \cos^2\theta \left[\Gamma_\uparrow + \Gamma_\downarrow - 2\Gamma_\varphi\right]$$
$$- \sin\theta \cos\theta \Gamma_\downarrow \left[\langle 1,N+1|\sigma|1,N+1\rangle \cos^2\theta + \langle 2,N+1|\sigma|2,N+1\rangle \sin^2\theta\right] +$$
$$\sin\theta \cos\theta \Gamma_\uparrow \left[\langle 1,N-1|\sigma|1,N-1\rangle \sin^2\theta + \langle 2,N-1|\sigma|2,N-1\rangle \cos^2\theta\right] -$$
$$\sin^2\theta \cos^2\theta \Gamma_\downarrow \left[\langle 1,N+1|\sigma|2,N+1\rangle + \langle 2,N+1|\sigma|1,N+1\rangle\right] -$$
$$\sin^2\theta \cos^2\theta \Gamma_\uparrow \left[\langle 1,N-1|\sigma|2,N-1\rangle + \langle 2,N-1|\sigma|1,N-1\rangle\right]$$

$$(72)$$

B. Steady state solution of Bloch equations (38), (39), (40)

The steady state solution $\rho^{(0)}$, $\rho_+^{(0)}$, $\rho_-^{(0)}$ of Bloch Eqs. (38), (39), (40) is found by equating of the left hand side of these equations to zero ($d\rho/dt = d\rho_+/dt = d\rho_-/dt = 0$). The result is as follows:

$$\rho^{(0)} = -\Gamma_- \left[\cos 2\theta \left(A_2 \Gamma_\varphi + \Omega_R^2\right) + B\Gamma_\varphi \sin 2\theta\right] / D \tag{73}$$

$$\rho_+^{(0)} = -\Gamma_- \Gamma_\varphi \left[A_1 \sin 2\theta + B \cos 2\theta\right] / D \tag{74}$$

$$\rho_-^{(0)} = -i\frac{\Omega_R}{\Gamma_\varphi}\rho_+^{(0)} \tag{75}$$

where

$$A_1 = \frac{1}{T_1}\cos^2 2\theta + \Gamma_\varphi \sin^2 2\theta \tag{76}$$

$$A_2 = \frac{1}{T_1}\sin^2 2\theta - \Gamma_\varphi \cos^2 2\theta \tag{77}$$

$$B = \left(\Gamma_\varphi - \frac{1}{T_1}\right)\sin 2\theta \cos 2\theta \tag{78}$$

$$D = \Gamma_\varphi^2 \left[2\sin^2 2\theta \cos^2 2\theta \left(\Gamma_\varphi - \frac{1}{T_1}\right) + \frac{1}{T_1}\cos 4\theta\right] - \Omega_R^2 \left(\frac{1}{T_1}\cos^2 2\theta + \Gamma_\varphi \sin^2\theta\right) \tag{79}$$

[1] I. I. Rabi, Phys. Rev. **51**, 652 (1937).
[2] Atomic and Molecular Beams: The State of The Art 2000, (Roger Compargue, ed.) Springer Verlag Telos, 2001.
[3] J. M. Raimond, M. Brune, and S. Haroche, Rev. Mod. Phys. **73**, 565 (2001).
[4] Makhlin Y. Schon G. and Shnirman A., Rev. Mod. Phys., 73 (2001) 357.
[5] D. V. Averin, in: *Exploring the quantum/classical frontier: recent advances in macroscopic quantum phenomena*, Ed. by J.R. Friedman and S. Han, (Nova Publishes, Hauppauge, NY, 2002), p. 441; cond-mat/0004364.
[6] A.N. Korotkov and D.V. Averin, Phys. Rev. B **64**, 165310 (2001).
[7] A.N. Korotkov, Phys. Rev. B **63**, 115403 (2001).

[8] Y. Nakamura, Yu.A. Pashkin, and J.S. Tsai., Phys. Rev. Lett. **87**, 246601 (2001).

[9] D. Vion et al., Science **296**, 886 (2002).

[10] J.M. Martinis, S. Nam, J. Aumentado, C. Urbina, Phys. Rev. Lett. **89**, 117901 (2002).

[11] I. Chiorescu et al., Science **299**, 1869 (2003).

[12] E. Ilichev, A.Yu. Smirnov, M. Grajcar, A. Izmalkov, D. Born1, N. Oukhanski, Th. Wagner, W. Krech, H.-G. Meyer, and A. Zagoskin, Fizika Nizkikh Temperatur, **30**, 823 (2004).

[13] E. Ilichev, N. Oukhanski, A. Izmalkov, Th. Wagner, M. Grajcar, H.-G. Meyer, A.Yu. Smirnov, A. Maassen van den Brink, M.H.S. Amin, A.M. Zagoskin, Phys. Rev. Lett. 91, 097906 (2003).

[14] A. Yu. Smirnov, Phys. Rev. B **68**, 134514 (2003).

[15] A. Yu. Smirnov, e-print archive cond-mat/0306004.

[16] Ju. Hauss, Rabi Spektroskopie an Qubit-Oszillator Systemen, Diploma thesis, Karlsruhe University, 2006.

[17] Ya. S. Greenberg and E. Ilichev, e-print archive quant-ph/0502187.

[18] Ya. S. Greenberg, E. Ilichev and A. Izmalkov, Europhys. Lett., **72**, 880 (2005)

[19] C. Coen-Tannoudji, J. Dupont-Rock, G. Grynberg, Atom-Photon Interactions. Basic Prinsiples and Applications. (John Wiley and Sons, 1998).

[20] Grifoni M. and Hanggi P., Phys. Rep., 304 (1998) 229.

[21] Frequently, the term "Rabi frequency" is associated with the quantity Ω_1. Here we call by this term the quantity Ω_R, the frequency with which the population oscillates if the high frequency detuning δ is different from zero.

[22] This statement about $\langle \sigma_x \rangle$ and $\langle \sigma_x \rangle$ is valid only as long as we neglect the transitions between the neighbor manifolds, which give the additional terms to the wave functions $|1, N\rangle$, $|2, N\rangle$. See Eqs. (9), (10).

Flux qubit as a sensor for a magnetometer with quantum limited sensitivity

E. Il'ichev[1],[*] and Ya. S. Greenberg[2]

[1]Institute for Physical High Technology, P.O. Box 100239, D-07702 Jena, Germany
[2]Novosibirsk State Technical University, 20 K. Marx Ave., 630092 Novosibirsk, Russia.
(Dated: August 21, 2006)

We propose to use the quantum properties of a superconducting flux qubit in the construction of a magnetometer with quantum limited sensitivity. The main advantage of a flux qubit is that its noise is rather low, and its transfer functions relative to the measured flux can be made to be about $10\text{mV}/\Phi_0$, which is an order of magnitude more than the best value for a conventional SQUID magnetometer. We analyze here the voltage-to-flux, the phase-to-flux transfer functions and the main noise sources. We show that the experimental characteristics of a flux qubit, obtained in recent experiments, allow the use of a flux qubit as magnetometer with energy resolution close to the Planck constant.

PACS numbers: 74.50.+r, 84.37.+q, 03.67.-a

Josephson-junction qubits are known to be candidates for solid-state quantum computing circuits[1]. However, owing to their unique quantum properties these devices undoubtedly can be used as sensitive detectors of different physical quantities, such as quantum environmental noise[2] or low frequency fluctuations of the junction critical current[3]. Here we propose to use a Josephson-junction flux qubit as a sensitive detector of magnetic flux[4]. We show that the present state-of-art allows one to obtain the energy sensitivity of such a detector in the order of the Planck constant.

A flux qubit[5,6,7] consists of three Josephson junctions in a loop with very small inductance L, typically in the pH range. This ensures an effective decoupling from the environment. Two junctions have an equal critical current I_c and (effective) capacitance C, while those of the third junction are slightly smaller: αI_c and αC, with $0.5 < \alpha < 1$. At sufficiently low temperatures (typically $T \approx (10 \sim 30)$ mK) when Φ_x, the external flux applied to the qubit loop, is in the close vicinity of $\Phi_0/2$ ($\Phi_0 = h/2e$ is the flux quantum, h is the Planck constant) the system has two low-lying quantum states E_- and E_+. The energy gap of the flux qubits, $\Delta/h = (E_+ - E_-)/h$ is of the order of several GHz. Below we assume $k_B T << \Delta$ (k_B is the Boltzmann constant), so that the qubit is definitely in its ground state E_-[8].

For experimental characterization the flux qubit is inductively coupled through a mutual inductance M to an LC tank circuit with known inductance L_T, capacitance C_T, and quality Q (Fig. 1).
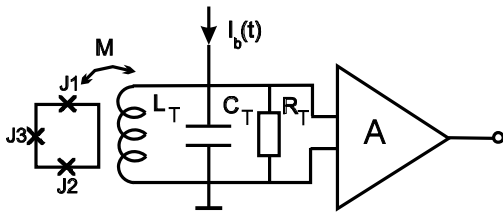

FIG. 1: Flux qubit coupled to a tank.

The resonant characteristics of the tank circuit (frequency, phase shift, etc.) are sensitive to the qubit inductance and therefore to the external flux Φ_x.

It was shown in[9] that the amplitude v and the phase χ of the output signal $V(t) = v\cos(\omega t + \chi)$ are coupled by the equations:

$$v^2\left(1 + 4Q^2\xi^2(f_x)\right) = I_0^2\omega_T^2 L_T^2 Q^2 \tag{1}$$

$$\tan\chi = 2Q\xi(f_x), \tag{2}$$

where I_0 is the amplitude of the driving current ($I_b(t) = I_0\cos\omega t$), and ω and ω_T are a driving frequency and the resonant frequency of the tank circuit, respectively.

It is worth noting that the the scheme in Fig. 1 and Eqs. (1), (2) are quite similar to those for a conventional RF SQUID. The only difference is in the expression for a flux-dependent frequency detuning $\xi(f_x)$. This depends on the qubit parameters as[9]:

$$\xi(f_x) = \xi_0 - k^2\frac{LI_c^2}{\Delta}\left(\frac{\lambda}{2\pi}\right)^2 F(f_x), \tag{3}$$

$\xi_0 = (\omega_T - \omega)/\omega_T$, $f_x = \Phi_x/\Phi_0 - \frac{1}{2}$, and

$$F(f_x) = \frac{1}{\pi}\int_0^{2\pi} d\phi \frac{\cos^2\phi}{\left[1 + \eta^2\left(f_x + \gamma\sin\phi\right)^2\right]^{3/2}}, \tag{4}$$

with $\eta = 2E_J\lambda/\Delta$ and $\gamma = MI_0Q/\Phi_0$. The expression for λ, which depends on α, I_C and C is given in[9].

Therefore, the main effect of the qubit-tank interaction is a shift of the tank resonance. This results in a dip in the voltage-to-flux and phase-to-flux characteristics which have been confirmed by experiments[10].

Theoretical phase-to-flux $\chi(f_x)$ (PFC) and voltage-to-flux (VFC) $v(f_x)$ dependencies at resonance $\omega = \omega_T$, are shown in Fig. 2 for three values of the amplitude of the bias current I_0. The graphs hasve been calculated from
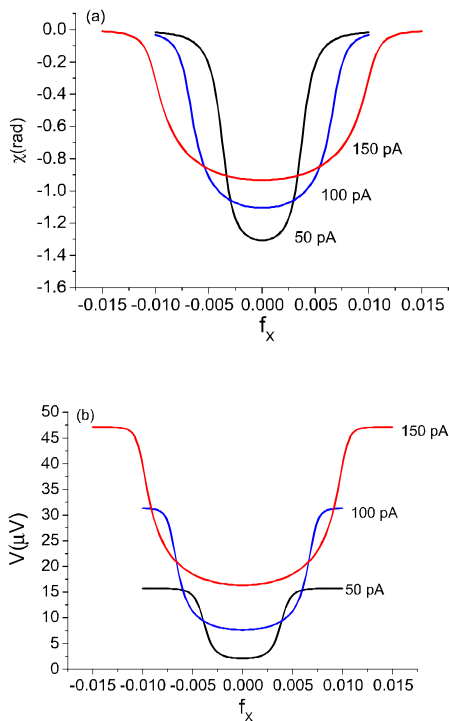
FIG. 2: (Color online). Tank phase χ (a) and tank voltage V (b) vs bias flux f_x for three values of bias current I_0. The gap frequency $\Delta/h = 2\text{GHz}$.

FIG. 3: (Color online). Phase-to-flux χ_Φ (a) and voltage-to-flux V_Φ (b) transfer functions for three values of bias current I_0. The gap frequency $\Delta/h = 2\text{GHz}$.

Eqs.(1), (2) for the following qubit-tank parameters: $I_c = 400$ nA, $\alpha = 0.8$, $L = 40$ pH, $L_T = 50$ nH, $Q = 10000$, $\omega_T/2\pi = 100$ MHz, $\Delta/h = 2$GHz, and $k = 10^{-2}$.

The advantage of a qubit magnetometer over a conventional SQUID magnetometer is in the very steep dependence of its VFC and PFC. In the flux locked loop operation of a magnetometer the working point is set at a fixed value of Φ_X where the slope of VFC or PFC is maximum. The output signal δV is proportional to the change $\delta\Phi_X$ of the measured flux. In principle two modes of detection are possible: voltage mode, where $\delta V = V_\Phi \delta\Phi_X$, and the phase mode, where $\delta V = \chi_\Phi \delta\Phi_X$. The qubit transfer functions $\chi_\Phi = v\partial\chi/\partial\Phi_X$ and $V_\Phi = \partial v/\partial\Phi_X$ are shown in Fig. 3 for the same qubit-tank parameters as those used in Fig. 2. It is seen that qubit transfer functions can exceed 10 mV/Φ_0. This value should be compared with 1 mV/Φ_0, the best value obtained for a DC SQUID with additional positive feedback[12].

The flux and energy sensitivity depend on the main noise sources, which come from the low frequency fluctuations of the junction critical current, S_{I_C}, and from the voltage noise, S_V and the current noise, S_I of the preamplifier, where S_{I_C}, S_V and S_I are the corresponding spectral densities. The fluctuations of I_C result in the fluctuating flux in the qubit loop $S_{\Phi,I_C}^{1/2} = LS_{I_C}^{1/2}$. For
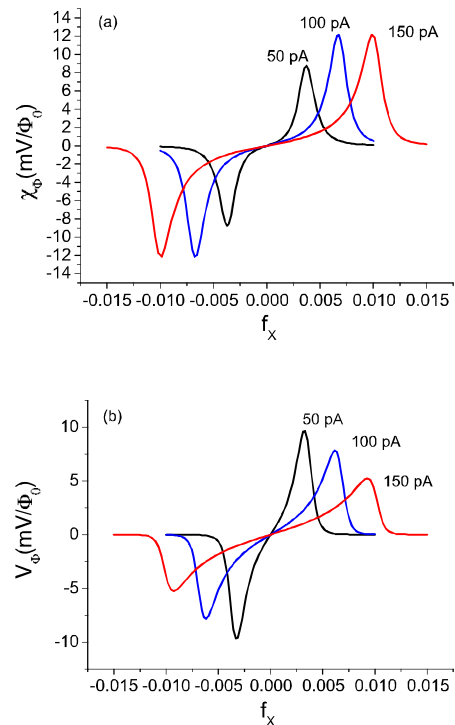
$I_C = 400$ nA, junction area $A = 0.12\mu\text{m}^2$, $T = 0.1$ K we estimate for three-junction flux qubit (see Eq.18 in[3]) $S_{\Phi,I_C}^{1/2} \approx 2 \times 10^{-8}\Phi_0/\text{Hz}^{1/2}$ at 1 Hz. We will see that this value is almost one order of magnitude smaller than the noise from a preamplifier. Therefore, the self noise of the qubit can be neglected. The contribution of the voltage noise of the preamplifier to the flux resolution referred to the input is $S_\Phi^V = S_V/V_\Phi^2$ or $S_\Phi^V = S_V/\chi_\Phi^2$ depending on the detection mode. The current noise of preamplifier which is related to its noise temperature T_N, $S_I = 4k_B T_N/R_T$, $(R_T = \omega_T L_T Q)$, contributes via two mechanisms. The first one comes from magnetic coupling between the tank inductance and the inductance of the qubit loop $S_\Phi^I = M^2 Q^2 S_I$. This contribution cannot be separated from the measured flux. The second mechanism contributes through a voltage noise induced by the current noise of the preamplifier across the dynamic resistance of the tank $S_\Phi^D = R_D^2 S_I/V_\Phi^2$ (or $S_\Phi^D = R_D^2 S_I/\chi_\Phi^2$), where $R_D = \partial v/\partial I_0$. By combining these three mechanisms we obtain for the flux sensitivity:

$$S_\Phi = M^2 Q^2 S_I + S_V/V_\Phi^2 + R_D^2 S_I/V_\Phi^2 \qquad (5)$$

where R_D is approximately equal to R_T, the resistance of unloaded tank. In the case of the phase mode detection we should substitute in (5) χ_Φ for V_Φ.
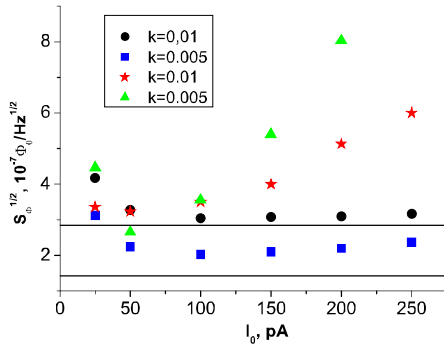
FIG. 4: (Color online). Flux sensitivity of qubit magnetometer. Phase detection mode is shown by boxes and circles. The stars and triangles are for the voltage detection. Two straight lines show the level of $S_{\Phi,1}$ for $k = 0.01$ (upper line) and $k = 0.005$ (lower line).

For the estimation we take $S_V^{1/2} = 0.2$ nV/Hz$^{1/2}$, and $T_N = 0.1$K[11], with the other parameters being the same as for Figs. 2, 3. The inspection of Eq. (5) shows that the main contribution to the flux noise comes from the first term:

$$S_{\Phi,1} = M^2 Q^2 S_I = k^2 Q \frac{4k_B T_N L}{\omega_T} \qquad (6)$$

This contribution does not depend on the position of the working point and for our parameters it gives $S_{\Phi,1}^{1/2} = 2.8 \times 10^{-7}\Phi_0$/Hz$^{1/2}$. The influence of the last two terms

in Eq. (5) depends on the position of the working point and on the bias current amplitude I_0. In general, the contribution of these terms is nonnegligible. The total flux noise dependence on the amplitude of bias current is shown in Fig. 4. As seen from the figure phase detection in general is more favorable than voltage detection. It gives lower noise and is weakly sensitive to I_0. The flux resolution can be improved by a decrease of $S_{\Phi,1}$ (see Eq. (6)) upon optimization of k, Q, ω_T, or L. However, it does not necessarily lead to a decrease of the total noise, since the transfer functions also depend on these parameters. (See, for example, the $k = 005$ curve in Fig. 4 for voltage detection). An increase of the bias frequency ω_T can also give an improved flux resolution. However, for the qubit to remain in the ground state the condition $\omega_T << \Delta/h$ should hold. We also made calculations for $\omega_T = 200$MHz with k=0.01, Q=1000, with other parameters being unchanged. We obtain at $I_0 = 200$pA for the phase detection $S_\Phi^{1/2} = 1.6 \times 10^{-7}\Phi_0$/Hz$^{1/2}$, which for $L = 40$pH corresponds to the energy sensitivity $\varepsilon = S_\Phi/2L = 1.3 \times 10^{-33}$J/Hz=2$h$. These values should be compared with those for conventional SQUIDs: $S_\Phi^{1/2} \approx 10^{-6}\Phi_0$/Hz$^{1/2}$, $\varepsilon \approx 10^{-32}$J/Hz[13].

In summary, we have shown that a superconducting flux qubit can be developed as a sensor of magnetic flux with an energy sensitivity close to the Planck constant.

* Electronic address: ilichev@ipht-jena.de
[1] Yu. Makhlin, G. Schön, and A. Shnirman, Rev. Mod. Phys. 73, 357 (2001).
[2] O. Astafiev, Y. A. Pashkin, Y. Nakamura, T. Yamamoto, and J. S. Tsaj, Phys. Rev. Lett. 93, 267007 (2004).
[3] D. J. Van Harlingen, T. L. Robertson, B. L. T. Plourde, P. A. Reichardt, T. A. Crane, and John Clarke, Phys. Rev. B 70, 064517 (2004).
[4] A similar idea has been considered in the work of V. I. Shnyrkov and S. I. Mel'nik (to be published in Fizika Nizkikh Temperatur (Low Temp. Phys.) 1, (2007), Kharkov, Ukraine). As distinct from our proposal, they studied a single junction interferometer with nonsinusoidal current phase relation. No estimations of the transfer functions or flux sensitivity were given.
[5] T.P. Orlando, J.E. Mooij, L. Tian, C.H. van der Wal, L. Levitov, S. Lloyd, and J.J. Mazo, Phys. Rev. B 60, 15398 (1999).
[6] J.E. Mooij, T.P. Orlando, L. Levitov, L. Tian, C.H. van der Wal, and S. Lloyd, Science 285, 1036 (1999).
[7] C.H. van der Wal, A.C.J. ter Haar, F.K. Wilhelm, R.N. Schouten, C.J.P.M. Harmans, T.P. Orlando, S. Lloyd, and J.E. Mooij, Science 290, 773 (2000).
[8] In principle, this condition can be sufficiently relaxed. In Ref. 9. it was shown that when the temperature was increased from $T = 10$ mK to $T = 200$ mK the width of the phase dip and therefore the steepness of the phase curve remained unchanched.
[9] Ya. S. Greenberg, A. Izmalkov, M. Grajcar, E. Il'ichev, W. Krech, H.-G. Meyer, M. H. S. Amin, and A. Maassen van den Brink, Phys. Rev. B 66, 214525 (2002).
[10] M. Grajcar, A. Izmalkov, E. Il'ichev, Th. Wagner, N. Oukhanski, U. Hubner, T. May, I. Zhilyaev, H. E. Hoenig, Ya. S. Greenberg, , V. I. Shnyrkov, D. Born, W. Krech, H.-G. Meyer, A. Maassen van den Brink, and M. H. S. Amin, Phys. Rev. B 69, 060501(R) (2004).
[11] N. Oukhanski, M. Grajcar, E. Il'ichev, and H.-G. Meyer, Rev. Sci. Instr. 74, 1145 (2003).
[12] D. Drung Supercond. Sci. Technol. 16, 1320 (2003).
[13] The SQUID Handbook, edited by J. Clarke and A. I. Braginski, Fundamentals and Technology of SQUIDs and SQUID Systems (Wiley-VCH, Weinheim, 2004), Vol. I.